KSME

Springer

Journal of Mechanical Science and Technology 38 (9) 2024

Original Article
DOI 10.1007/s12206-024-0807-4

Keywords:
· Component mode synthesis
· Fixed interface
· Geometric nonlinearity
· Non-intrusive model order reduction
· Review

Correspondence to:
Jun-Sik Kim
junsik.kim@kumoh.ac.kr

Citation:
Bui, T. A., Park, J., Kim, J.-S. (2024). A review of combining component mode synthesis and model order reductions for geometrically nonlinear analysis. Journal of Mechanical Science and Technology 38 (9) (2024) 4699~4711.
http://doi.org/10.1007/s12206-024-0807-4

Received January 23rd, 2024
Revised April 18th, 2024
Accepted May 13th, 2024

† Recommended by Editor
No-cheol Park

A review of combining component mode synthesis and model order reductions for geometrically nonlinear analysis

Tuan Anh Bui[1], Junyoung Park[1,2] and Jun-Sik Kim[1,2]

[1]Department of Aeronautic, Mechanical and Electrical Convergence Engineering, Kumoh National Institute of Technology, 61 Daehak-ro, Gumi, Gyeongbuk 39177, Korea, [2]School of Mechanical System Engineering, Kumoh National Institute of Technology, 61 Daehak-ro, Gumi, Gyeongbuk 39177, Korea

Abstract This paper reviews the recent advances on the combination of component mode synthesis and model order reduction for geometrically nonlinear analysis, focusing on fixed-interface substructures and non-intrusive reduced-order models. These approaches offer significant potential for engineering applications by enabling accurate mechanical behavior prediction without detailed geometric and material information. Additionally, they facilitate safe sharing and collaboration between companies, reducing design times and production costs while also offering computational efficiency. However, challenges remain, indicating the need for future improvements in this area.

1. Introduction

Designing complex structures such as airplanes, ships, and automobiles is a challenging and time-consuming process. To reduce the design time and improve the design quality, the entire structure is often divided into multiple substructures and assigned to different departments. This approach enables parallel processing and allows multiple teams to work on different parts of the structure simultaneously, which significantly reduces the overall design time. Additionally, it allows each department to focus on specific substructures and become experts in their respective areas, resulting in improved overall design quality [1, 2].

To further reduce design time, model order reduction techniques can be applied to substructures. This involves constructing reduced-order models (ROM) for the substructures, which are then assembled to form a ROM of the entire structure. The ROM has a significantly lower computational cost than the finite element (FE) model, especially in simulations of structural dynamics.

Furthermore, a ROM has an advantage over a FE model in that it does not require geometry and material information of the structure. This can be particularly important in projects involving multiple independent companies, such as collaborations between an original equipment manufacturer and its partners. Each company is responsible for designing and manufacturing specific components of the structure. ROMs of these components can be securely shared between companies for design optimization purposes.

The structure of vehicles is often made as thin as possible to reduce weight, thereby improving energy efficiency [3–5]. In such cases, the structure is allowed to undergo large displacements, as long as the material still remains elastic. However, striking a balance between economy and safety presents a challenge that requires geometrically nonlinear analysis. Therefore, the development of nonlinear ROMs has become necessary and has attracted the attention of many scientists in recent years.

The objective of this paper is to provide a review of recent advances in the combination of component mode synthesis and model order reduction techniques for substructures. The process of constructing ROMs for substructures is shown in Fig. 1. The remainder of this paper is organized as follows: Sec. 2 provides an overview of component mode synthesis, Sec. 3 cov-

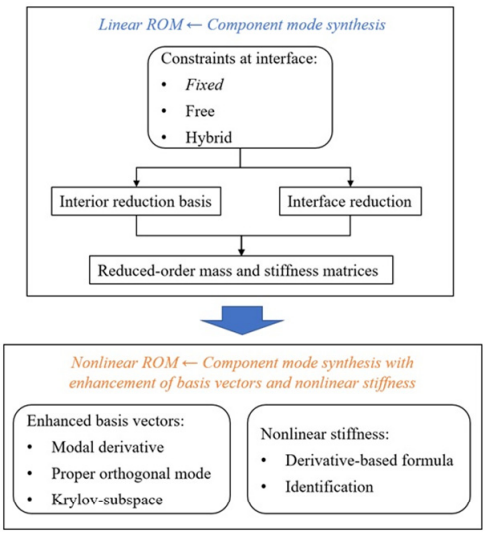

Fig. 1. Flow chart for the correction of the roll forming process design.

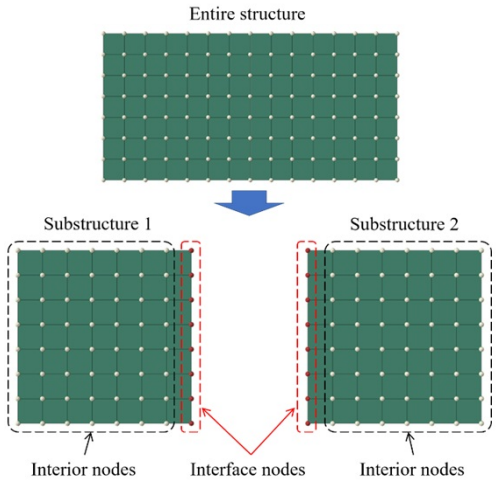

Fig. 2. The division of the entire structure into two substructures.

ers geometrically nonlinear ROM, Sec. 4 evaluates the combination of component mode synthesis and ROM, and Sec. 5 presents conclusions and perspectives.

2. Component mode synthesis

2.1 Overview of component mode synthesis

Component mode synthesis was initially introduced for linear dynamic analysis of complex and discontinuous geometric structures, which could not be effectively simulated due to their high number of degrees of freedom (DOFs) [2]. Component mode synthesis addresses such structures by dividing them into several components that are geometrically simpler or contain a limited number of DOFs for processing (see Fig. 2), and then reassembling them later. Recognizing the potential of component mode synthesis, the research community collaborated to further develop this method. Today, it is commonly used to address structures that are discontinuous in both geometry and materials. Structures with local nonlinearities, such as contact or material nonlinearities, can be divided into linear and nonlinear components for processing, thereby keeping computational costs reasonable.

Component mode synthesis is built on the assumption that the physical displacement of substructures is a linear combination of a small number of vibration modes and static modes. This assumption is effective because high-frequency vibration modes contribute very little to the dynamic behavior of structures.

There are three approaches in component mode synthesis techniques concerning the constraints at the interface of substructures: fixed [6, 7], free [8, 9], and hybrid [10, 11]. This paper focuses on the fixed interface approach because of its simplicity and robustness, which has made it widely adopted in engineering [12–23].

Commercial FE software, such as Abaqus and Nastran, includes the fixed interface component mode synthesis. However, it still has certain limitations. Firstly, it is not possible to apply force or displacement to the internal nodes of the substructure. Additionally, the stiffness and mass matrices of the substructure are assumed to be constant, which means that the substructure model cannot account for geometric nonlinearity. Unfortunately, these limitations are increasingly becoming necessary in the structural design process. While commercial FE software has not yet improved component mode synthesis techniques to address these shortcomings, users may need to develop their own code to overcome such limitations. In such case, the commercial FE software, as well as open-source software (e.g., Eigen, SLEPc), can be used to extract eigenvalues and eigenvectors, serving to build nonlinear ROMs for substructures.

2.2 Linear projection onto a smaller-dimensional space

The linear equation of motion (undamped) for a substructure is as follows [1]:

$$\mathbf{M}_s\ddot{\mathbf{u}}_s + \mathbf{K}_s\mathbf{u}_s = \mathbf{f}_s + \mathbf{g}_s \,, \tag{1}$$

in which the subscript s denotes the substructure. $\mathbf{M}$ represents the mass matrix, $\mathbf{K}$ the linear stiffness matrix, $\mathbf{u}$ the nodal displacement vector, $\mathbf{f}$ the external force, and $\mathbf{g}$ the connecting force between substructures. The nodal displacement vector, which includes N DOFs, can be reduced in size by projecting onto a smaller-dimensional space as follows [1]:

$$\mathbf{u}_s = \mathbf{V}_s\mathbf{q}_s \,, \tag{2}$$

where $\mathbf{q}_s$ is a vector consisting of n generalized coordinates, and $\mathbf{V}_s$ is a reduction basis ($\mathbf{V}_s \in \Re^{N\times n}$). Eq. (1) is then reduced in size as follows:

$$\left(\mathbf{V}_s^T\mathbf{M}_s\mathbf{V}_s\right)\ddot{\mathbf{q}}_s+\left(\mathbf{V}_s^T\mathbf{K}_s\mathbf{V}_s\right)\mathbf{q}_s=\mathbf{V}_s^T\left(\mathbf{f}_s+\mathbf{g}_s\right). \tag{3}$$

Consequently, the choice of the reduction basis is crucial because it directly influences the accuracy and computational cost of the linear ROM.

The substructure's nodes can be distinguished between interface nodes (denoted by the superscript B) and interior nodes (denoted by the superscript I), as shown in Fig. 2. Eq. (1) can be rewritten with the decomposition of the interface DOFs and the interior DOFs as follows [7]:

$$\begin{bmatrix}\mathbf{M}_s^{BB} & \mathbf{M}_s^{BI}\\ \mathbf{M}_s^{IB} & \mathbf{M}_s^{II}\end{bmatrix}\begin{bmatrix}\ddot{\mathbf{u}}_s^B\\ \ddot{\mathbf{u}}_s^I\end{bmatrix}+\begin{bmatrix}\mathbf{K}_s^{BB} & \mathbf{K}_s^{BI}\\ \mathbf{K}_s^{IB} & \mathbf{K}_s^{II}\end{bmatrix}\begin{bmatrix}\mathbf{u}_s^B\\ \mathbf{u}_s^I\end{bmatrix}=\begin{bmatrix}\mathbf{f}_s^B+\mathbf{g}_s\\ \mathbf{f}_s^I\end{bmatrix}. \tag{4}$$

Typically, reducing the number of interior DOFs is given priority since their count is usually greater than that of interface DOFs. Nevertheless, the number of interface DOFs can be significant in some cases, and researchers have also proposed several methods to reduce their count.

To reduce the DOFs of substructures, it is necessary to consider constraints at the interface. These interface constraints can take different forms, such as fixed [6, 7], free [8, 9], or hybrid [10, 11]. In this section, we provide a brief overview of the fixed interface method, which is widely adopted in engineering [24–26]. With the fixed interface approach, the connecting force between the substructures ($\mathbf{g}_s$) is not taken into account during the assembly of ROMs for the substructures, because they mutually cancel each other out. For a more detailed exploration of other approaches, please refer to Refs. [1, 2, 27-29].

2.3 Reducing interior DOFs

For the fixed interface approach, the displacement of the interior nodes depends on the displacement of the interface nodes and the generalized interior coordinates, as suggested by Ref. [7]. The relationship is as follows:

$$\mathbf{u}_s^I\approx\mathbf{\Psi}_s\mathbf{u}_s^B+\mathbf{\Phi}_s\mathbf{q}_s^I\ , \tag{5}$$

where $\mathbf{q}_s^I$ is a vector consisting of generalized interior coordinates. $\mathbf{\Psi}_s$ is a matrix consisting of constraint modes. The number of constraint modes is equal to the number of interface DOFs. By giving each interface DOF a unit displacement while fixing the remaining interface DOFs, one can obtain a corresponding constraint mode, as illustrated in Fig. 3. The constraint modes can be computed as follows [7]:

$$\mathbf{\Psi}_s=-\left(\mathbf{K}_s^{II}\right)^{-1}\mathbf{K}_s^{IB}. \tag{6}$$

$\mathbf{\Phi}_s$ is a matrix consisting of selected vibration modes. Fig. 3 illustrates a vibration mode of a substructure with the fixed constraint at the interface. The vibration modes are obtained by solving the eigenvalue equation of the substructure, as below

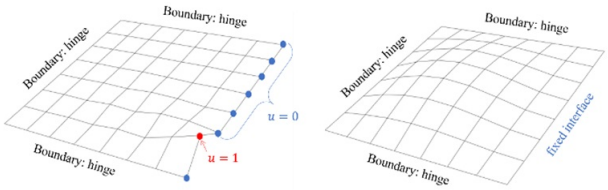

Fig. 3. A constraint mode (left) and a vibration mode (right) of a plate with fixed interface.

[7]:

$$\left(\mathbf{K}_s^{II}-\omega_{s,i}^2\mathbf{M}_s^{II}\right)\mathbf{\Phi}_{s,i}=\mathbf{0}\ . \tag{7}$$

Thus, the reduction basis of the substructure model is as follows [7]:

$$\begin{bmatrix}\mathbf{u}_s^B\\ \mathbf{u}_s^I\end{bmatrix}\approx\begin{bmatrix}\mathbf{I} & \mathbf{0}\\ \mathbf{\Psi}_s & \mathbf{\Phi}_s\end{bmatrix}\begin{bmatrix}\mathbf{u}_s^B\\ \mathbf{q}_s^I\end{bmatrix} \tag{8}$$

where $\mathbf{I}$ is an identity matrix.

2.4 Reducing interface DOFs

Today, structural models often try to describe the physics as closely to reality as possible. Consequently, the size of FE models is increasing. While the number of interior DOFs has been reduced, the number of interface DOFs remains significant in certain cases. Therefore, the reduction of interface DOFs has been proposed by Craig and Chang since 1977 [30]. However, it is only in recent years that this task has garnered significant attention from researchers [31–38].

The reduction of interface DOFs can be performed on the model of the entire structure (global level) or on each model of the substructures (local level). In both cases, the displacement at the interface is approximated by a linear combination of a small number of eigenvectors (referred to as the characteristic constraint modes by Ref. [31]) as follows:

$$\mathbf{u}^B\approx\mathbf{\Phi}^{CC}\mathbf{q}^B\ , \tag{9}$$

where $\mathbf{q}^B$ is a vector consisting of generalized interface coordinates. $\mathbf{\Phi}^{CC}$ is a matrix consisting of selected characteristic constraint modes.

The characteristic constraint modes can be calculated at the global level as follows [31]:

$$\left(\mathbf{K}^{BB}-\omega_i^2\mathbf{M}^{BB}\right)\mathbf{\Phi}_i^{CC}=\mathbf{0}\ , \tag{10}$$

in which $\mathbf{K}^{BB}$ and $\mathbf{M}^{BB}$ are the stiffness and mass matrices of the interface part in the model of entire structure, respectively.

Computing the characteristic constraint modes at the global level must be performed after assembling the models of all

substructures into a single model of the entire structure. It may be cumbersome if the entire structure is divided into numerous substructures. Therefore, the characteristic constraint modes have been proposed to compute at the local level in several studies [32, 36, 37].

The characteristic constraint modes can be calculated at the local level as follows [36]:

$$\left(\mathbf{K}_s^{BB} - \omega_{s,i}^2 \mathbf{M}_s^{BB}\right)\boldsymbol{\Phi}_{s,i}^{CC} = \mathbf{0}\,, \tag{11}$$

in which $\mathbf{K}_s^{BB}$ and $\mathbf{M}_s^{BB}$ are the stiffness and mass matrices of the interface part in the model of substructure, respectively. The reduction basis for the fixed-interface model, including the reduction of the interface DOFs, is calculated as follows:

$$\begin{bmatrix}\mathbf{u}_s^B \\ \mathbf{u}_s^I\end{bmatrix} \approx \left(\begin{bmatrix}\mathbf{I} & \mathbf{0} \\ \boldsymbol{\Psi}_s & \boldsymbol{\Phi}_s\end{bmatrix}\begin{bmatrix}\boldsymbol{\Phi}_s^{CC} & \mathbf{0} \\ \mathbf{0} & \mathbf{I}\end{bmatrix}\right)\begin{bmatrix}\mathbf{q}_s^B \\ \mathbf{q}_s^I\end{bmatrix}. \tag{12}$$

The reduction of local-level interface DOFs is performed on each substructure prior to assembly, making it very convenient for subsequent assembly. When assembling two models of two substructures connected by an interface, the same characteristic constraint modes must be used for both models. However, in the case of an interface with complex geometry, the characteristic constraint modes of adjacent substructures may not be the same. In such cases, one might need to apply methods such as singular value decomposition [32, 36, 39], weak compatibility [32, 35], or uncoupled weak compatibility [32] to ensure that the local characteristic constraint modes of adjacent substructures are identical.

In addition, the reduction of interface DOFs has also been successfully performed for other interface constraint methods. For more details, one can refer to the Refs. [11, 40, 41].

3. Nonlinear ROM for substructure

3.1 Overview of geometrically nonlinear ROMs

When the structure vibrates with large amplitude, the assumption of a linear relationship between displacement and load becomes invalid, making linear analysis inaccurate. In such cases, analyzing geometric nonlinearity is necessary, requiring the recalculation of tangential stiffness and internal forces each time the structure's displacement changes. Geometrically nonlinear analysis has been recommended for aircraft engine design [42]. However, dynamic analysis often involves numerous iterations, thus considering geometric nonlinearity significantly increases computational cost.

Nonlinear ROM can be used to predict the geometrically nonlinear behavior of structures at low computational cost. To reduce computational cost, the number of DOFs of the model must be reduced by projecting the displacement vector onto a smaller-dimensional space. The projection from the physical displacement space to the reduced space can be linear or nonlinear (i.e., a quadratic manifold) [43]. In the context of substructures, linear projection is naturally compatible with component mode synthesis while the applicability of nonlinear projection is questionable, especially when considering interface reduction. Therefore, this study focuses on linear projection-based ROMs.

In geometrically nonlinear ROM, the nonlinear internal force of the structure is assumed to be a polynomial of the generalized coordinates. This assumption is derived from the Taylor series expansion of functions. The simplicity of calculating a polynomial is also a reason why this assumption is widely used.

The coefficients of the polynomial, referred to as nonlinear stiffness coefficients, can be computed by intrusive or non-intrusive methods, as classified in Ref. [44]. Non-intrusive methods do not require intervention in the source code of FE software. They only require the extraction of internal forces or displacement vectors; therefore, they are compatible with commercial FE software, leading to wide applicability in engineering. Therefore, this paper focuses on non-intrusive methods.

In geometrically nonlinear analysis, the nonlinear internal force component is considered, resulting in the equation of motion (undamped) for a substructure as follows [1]:

$$\mathbf{M}_s\ddot{\mathbf{u}}_s + \mathbf{K}_s\mathbf{u}_s + \boldsymbol{\Gamma}_s\left(\mathbf{u}_s\right) = \mathbf{f}_s + \mathbf{g}_s\,, \tag{13}$$

in which $\boldsymbol{\Gamma}$ represents the nonlinear component of internal force.

Two problems arise when constructing geometrically nonlinear ROMs [45]. The first problem is to build an efficient reduction basis that accurately represents the nonlinear displacement of the structure while minimizing the number of modes. The second problem involves reproducing the nonlinear internal force components of the structure within the ROM. These two problems are reviewed in the following two subsections.

3.2 Reduction basis

The reduction basis is a mapping between the displacements of the FE model and the generalized coordinates of the ROM. One can use linear or nonlinear mapping for geometrically nonlinear ROMs. Nonlinear mapping (manifold) methods have been reviewed in detail in the Ref. [43]. This paper focuses only on linear mapping due to its simplicity and robustness. This means that the model is still reduced in size according to Eqs. (2) and (3), but the reduction basis must be enhanced by some basis vectors to ensure the accuracy of the projection when dealing with geometric nonlinearities. The following subsections briefly review the basis vectors that have been proposed to enhance the reduction basis of substructure models.

3.2.1 Modal derivative

The modal derivative, which is the derivative of the eigenvector with respect to the generalized coordinates, was first proposed for nonlinear dynamics analysis by Idehlson and Cardo-

na [46, 47]. It is possible to compute the modal derivatives exactly, but the computational cost is high [48]. To reduce the cost, the modal derivatives can be approximated using Eq. (14) [46]. It should be noted that the derivative of the stiffness matrix with respect to the generalized coordinates can be calculated using the finite difference method. The modal derivative calculated in this way is called the static modal derivative, as it ignores the inertial components.

$$\boldsymbol{\Theta}_{ij} = \left.\frac{\partial \boldsymbol{\Phi}_i}{\partial \mathbf{q}_j}\right|_0 = -\left(\mathbf{K}\big|_0\right)^{-1} \left.\frac{\partial \mathbf{K}}{\partial \mathbf{q}_j}\right|_0 \boldsymbol{\Phi}_i \,. \tag{14}$$

More recently, the static modal derivatives have been used to enhance the reduction basis of nonlinear ROM of substructures [49–51]. The static modal derivatives may need to be modified to satisfy the constraint assumption at the interface. For example, in the case of a classical fixed-interface model, the static modal derivatives must be computed as follows [52]:

$$\boldsymbol{\Theta}_{s,ij} = -\left(\mathbf{K}_s^{II}\big|_0\right)^{-1} \left(\left.\frac{\partial \mathbf{K}_s^{II}}{\partial \gamma_{s,i}}\right|_0 \mathbf{X}_{s,j}^{I} + \left.\frac{\partial \mathbf{K}_s^{IB}}{\partial \gamma_{s,i}}\right|_0 \mathbf{X}_{s,j}^{B} \right), \tag{15}$$

in which $\boldsymbol{\gamma}_s = \left[\mathbf{u}_s^B \quad \mathbf{q}_s^I\right]^T$, $\mathbf{X}_s^I = \left[\boldsymbol{\Psi}_s \quad \boldsymbol{\Phi}_s\right]$, and $\mathbf{X}_s^B = \left[\mathbf{I} \quad \mathbf{0}\right]$. The reduction basis and the generalized coordinates will be further expanded as follows [52]:

$$\begin{bmatrix} \mathbf{u}_s^B \\ \mathbf{u}_s^I \end{bmatrix} \approx \begin{bmatrix} \mathbf{I} & \mathbf{0} & \mathbf{0} \\ \boldsymbol{\Psi}_s & \boldsymbol{\Phi}_s & \boldsymbol{\Theta}_s \end{bmatrix} \begin{bmatrix} \mathbf{u}_s^B \\ \mathbf{q}_s^I \\ \boldsymbol{\xi}_s^I \end{bmatrix}, \tag{16}$$

where $\boldsymbol{\xi}_s^I$ is extra coordinates, $\boldsymbol{\Theta}_s$ is a matrix that includes selected static modal derivatives.

By using a reduction basis as expressed in Eq. (16), the nonlinear ROM can accurately predict the mechanical behavior of the substructure under various load cases. This is possible because the linear vibration modes and static modal derivatives are independent of the applied load. However, the main challenge of this method lies in selecting the appropriate basis vectors to achieve a minimal reduction basis size while maintaining high projection accuracy. Several strategies have been proposed to address this challenge, involving the selection of necessary modes and the elimination of duplicated or unnecessary modes [53–56].

3.2.2 Proper orthogonal mode

Data-driven methods such as Proper orthogonal decomposition can be used to calculate the best-fit space for projection [42, 57–65]. Firstly, the substructure's nodal displacements at various time instances are stored in a matrix ($\mathbf{A}_s$) known as the snapshot matrix, as illustrated in Eq. (17). The proper orthogonal modes $\boldsymbol{\Phi}_s^{POD}$ are then obtained through the singular value decomposition of the snapshot matrix, as expressed in Eq. (18). These modes constitute a projection space where the projection error is minimized. To optimize the size of the reduction basis, only the modes with the largest corresponding singular values are selected, while the ones with small singular values can be discarded.

$$\mathbf{A}_s = \left[\mathbf{u}_s(t_1) \quad \mathbf{u}_s(t_2) \quad \cdots \quad \mathbf{u}_s(t_m)\right], \tag{17}$$

$$\mathbf{A}_s = \boldsymbol{\Phi}_s^{POD} \mathbf{Z} \mathbf{R}^T \,. \tag{18}$$

These modes may have non-zero displacements at interface nodes, as shown in Eq. (19). In such cases, it is necessary to modify these modes, as depicted in Eq. (20), to ensure zero displacement at the interface nodes [42]. Finally, the reduction basis of the substructure is expressed by Eq. (21).

$$\boldsymbol{\Phi}_s^{POD} = \begin{bmatrix} \boldsymbol{\Phi}_s^{POD,B} \\ \boldsymbol{\Phi}_s^{POD,I} \end{bmatrix}, \tag{19}$$

$$\tilde{\boldsymbol{\Phi}}_s^{POD,I} = \boldsymbol{\Phi}_s^{POD,I} - \boldsymbol{\Psi}_s \boldsymbol{\Phi}_s^{POD,B}, \tag{20}$$

$$\begin{bmatrix} \mathbf{u}_s^B \\ \mathbf{u}_s^I \end{bmatrix} \approx \begin{bmatrix} \mathbf{I} & \mathbf{0} \\ \boldsymbol{\Psi}_s & \tilde{\boldsymbol{\Phi}}_s^{POD,I} \end{bmatrix} \begin{bmatrix} \mathbf{u}_s^B \\ \mathbf{q}_s^I \end{bmatrix}. \tag{21}$$

The advantage of the reduction basis indicated in Eq. (21) is its relatively compact size. However, a drawback of this approach is the high computational cost associated with obtaining the snapshot matrix. Furthermore, when changing the type of load, it is necessary to recalculate the proper orthogonal modes.

3.2.3 Krylov-subspace

Another method to generate a reduction basis, which also uses information about the spatial distribution of the applied load, involves relying on Krylov-subspace [66]. Let's consider a linear equation of motion (undamped) for a structure, as shown in Eq. (22). The linear displacement of the structure can be approximated through a linear combination of static modes, as demonstrated in Eq. (23) [1, 67–72]. The first static mode represents the static displacements induced by external forces (Eq. (24)). The second static mode corresponds to the displacement of the structure under a pseudo load, which is the inertial force $\mathbf{M}\boldsymbol{\varphi}_1^{static}$. Consequently, the calculation of the i^{th} static mode is based on the previous static mode, as expressed in Eq. (25). To ensure mutual orthogonality in terms of mass and stiffness and to mitigate round-off errors, it is necessary to modify the static modes following the guidelines provided in the Refs. [1, 70].

$$\mathbf{M}\ddot{\mathbf{u}} + \mathbf{K}\mathbf{u} = \mathbf{f} \,, \tag{22}$$

$$\mathbf{u}_{linear} \approx \sum_{i=1}^{n} \boldsymbol{\varphi}_i^{static} \mathbf{q}_i \,, \tag{23}$$

$$\boldsymbol{\varphi}_1^{static} = \mathbf{K}^{-1}\mathbf{f} \,, \tag{24}$$

$$\boldsymbol{\varphi}_i^{static} = \mathbf{K}^{-1}\mathbf{M}\boldsymbol{\varphi}_{i-1}^{static} \,. \tag{25}$$

For geometrically nonlinear analysis, the modal derivatives of the static modes, which are also computed using Eqs. (14) and

(15), are further enriched for the reduction basis. The reduction basis of a substructure model is as follows:

$$\begin{bmatrix} \mathbf{u}_s^B \\ \mathbf{u}_s^I \end{bmatrix} \approx \begin{bmatrix} \mathbf{I} & \mathbf{0} & \mathbf{0} \\ \boldsymbol{\Psi}_s & \boldsymbol{\Phi}_s^{static} & \boldsymbol{\Theta}_s^{static} \end{bmatrix} \begin{bmatrix} \mathbf{u}_s^B \\ \mathbf{q}_s^I \\ \boldsymbol{\xi}_s^I \end{bmatrix} . \tag{26}$$

The Krylov-subspace offers several advantages compared to the linear vibration modes and the proper orthogonal modes. It requires a smaller subspace size to achieve similar projection accuracy compared to the linear vibration modes. Additionally, calculating the static modes can be more cost-effective than the vibration modes since it avoids the need to solve an eigenvalue problem, particularly for large-sized FE models. In contrast to the proper orthogonal modes, the computation of the static modes is less expensive as it only requires linear analysis, while generating the proper orthogonal modes necessitates nonlinear analysis. However, similar to the proper orthogonal modes, the Krylov-subspace shares the disadvantage of being load-dependent. Therefore, when the type of load changes, recalculating the Krylov-subspace becomes necessary.

3.3 Nonlinear stiffness coefficients

This section reviews methods for calculating nonlinear stiffness coefficients, which aid in reconstructing the nonlinear internal forces of the nonlinear ROM. The nonlinear stiffness coefficients can be computed using either intrusive methods (which necessitate permission to interfere the FE code) or non-intrusive methods (which do not require permission to interfere the FE code) [44]. This paper focuses on non-intrusive methods because they are compatible with commercial finite element software, thereby broadening their applicability in engineering.

3.3.1 Taylor-expansion-based stiffness

The internal force of the substructure can be approximated by a polynomial of generalized coordinates through a Taylor series expansion around the equilibrium position, as depicted in Refs. [73–75]:

$$\mathbf{f}_{\text{int}} \approx \left.\frac{\partial \mathbf{f}_{\text{int}}}{\partial \mathbf{q}}\right|_0 \mathbf{q} + \frac{1}{2!}\left.\frac{\partial^2 \mathbf{f}_{\text{int}}}{\partial \mathbf{q}^2}\right|_0 \mathbf{qq} + \frac{1}{3!}\left.\frac{\partial^3 \mathbf{f}_{\text{int}}}{\partial \mathbf{q}^3}\right|_0 \mathbf{qqq} + \dots . \tag{27}$$

Therefore, the internal force vector after size reduction is also approximated by a polynomial, as follows:

$$\mathbf{f}_{\text{int},red} = \mathbf{V}^T \mathbf{f}_{\text{int}} \approx \mathbf{K}^{(1)}\mathbf{q} + \mathbf{K}^{(2)}\mathbf{qq} + \mathbf{K}^{(3)}\mathbf{qqq} + \dots . \tag{28}$$

where the stiffness tensors are calculated as follows:

$$\mathbf{K}^{(1)} = \mathbf{V}^T \mathbf{K}\big|_0 \mathbf{V} , \tag{29}$$

$$\mathbf{K}^{(2)} = \frac{1}{2!}\mathbf{V}^T \left.\frac{\partial \mathbf{K}}{\partial \mathbf{q}}\right|_0 \mathbf{V} , \tag{30}$$

$$\mathbf{K}^{(3)} = \frac{1}{3!}\mathbf{V}^T \left.\frac{\partial^2 \mathbf{K}}{\partial \mathbf{q}^2}\right|_0 \mathbf{V} . \tag{31}$$

The derivatives of the stiffness matrix (or internal force vector) with respect to the generalized coordinates can be calculated using the central difference method. This method is compatible with commercial finite element software, offers good accuracy, and is cost-effective [73, 75].

In the case of the FE model of the structure generated based on the von Kármán or St. Venant-Kirchhoff theories, the internal force of the structure precisely follows a cubic polynomial of the physical coordinates as well as the generalized coordinates [74, 76–79]. However, in other cases, the cubic polynomial is merely an approximation, which may introduce varying degrees of error. Unfortunately, many commercial FE software packages do not employ these special theories, necessitating careful consideration of the polynomial order.

When using commercial FE software to construct a nonlinear ROM, representing the nonlinear internal forces with a cubic polynomial still produces satisfactory results in certain boundary conditions. These scenarios typically involve boundary conditions that restrict the in-plane displacement of the structure, such as clamped-clamped beams or fully clamped plates [73, 75]. However, if the in-plane displacement of the structure is significant, such as in the case of cantilever beams subjected to transverse loads, a cubic polynomial assumption is insufficient. In such cases, a fifth-order polynomial provides better results [73, 75]. Furthermore, it has been demonstrated that the use of a fifth-order polynomial also yields better results for curved beam substructures [80].

3.3.2 Identified stiffness

The nonlinear stiffness coefficients can also be identified by solving a system of linear algebraic equations, as shown in Eq. (32), where **x** is a vector containing the unknown stiffness coefficients. There are two strategies to obtain this system of equations. The first strategy involves imposing selected displacements on the structure, while the second strategy involves imposing selected loads on the structure.

$$\mathbf{Cx} = \mathbf{D} . \tag{32}$$

The first strategy includes two methods: Enforced displacement (ED) and enhanced enforced displacement (EED). In the ED method, the nonlinear stiffness coefficients are identified based on the static displacements and the corresponding internal forces [81, 82]. Meanwhile, in the EED method, the nonlinear stiffness coefficients are identified based on the static displacements and the corresponding tangent stiffness matrices of the structure [83, 84]. The process of these two methods is illustrated in Fig. 4.

To solve a system of linear equations, the number of equa-

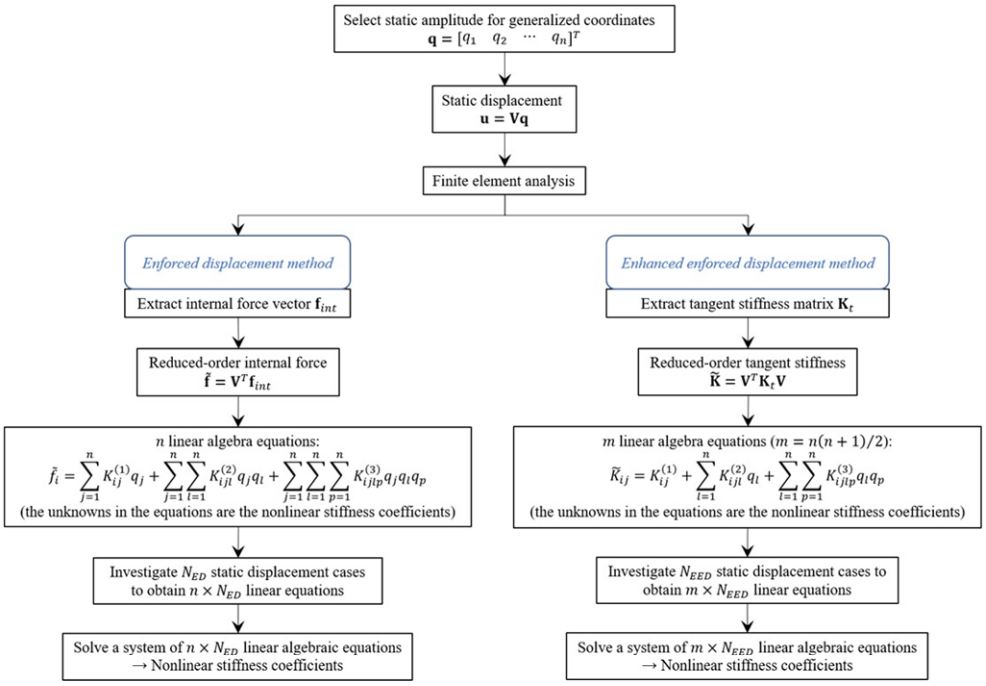

Fig. 4. Process of ED and EED identification methods.

tions must be greater than or equal to the unknowns. In each displacement case, the EED method obtains more equations than the ED method. Therefore, the number of calculation cases required by the EED method (N_{EED}) is fewer than that of the ED method (N_{ED}), resulting in a lower computational cost for the EED method compared to the ED method [45]. However, the ED method is compatible with most commercial FE software, while the EED method may not be feasible due to the potential inability to extract the tangent stiffness matrix with certain commercial FE software.

To ensure that the stiffness coefficients are always determined, sets of up to three equations are constructed and solved sequentially instead of solving a large system of equations. The construction of small equation sets is achieved by isolating a few generalized coordinates [45, 81–84]. Additionally, the choice of magnitude for the generalized coordinates during identification can impact the identified stiffness coefficients, which in turn influences the outcome of the ROM [76, 82, 85, 86]. Further details can be found in the Refs. [45, 81, 84, 85].

The second strategy, known as the implicit condensation and expansion (ICE) method, identifies the nonlinear stiffness coefficients based on the static loads and the corresponding displacements of the structure [87–92]. This method assumes that the membrane displacement of the structure is small, thereby having negligible influence on the internal forces. Consequently, the reduction base only includes transverse vibration modes. The internal force is assumed to be a cubic polynomial of the generalized coordinates associated with the transverse vibration modes. The coefficients of this polynomial are determined using least squares methods. In situations where the calculation of the membrane displacement is necessary to determine the structural stress, it can be calculated based on its assumed relationship with the transverse displacement.

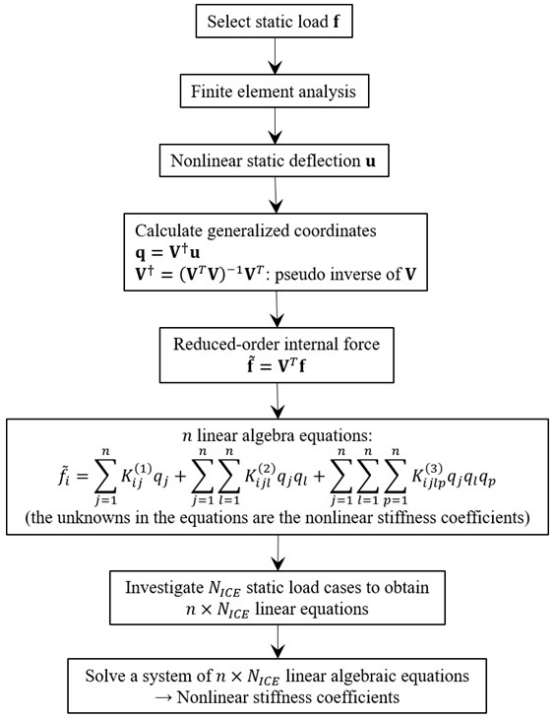

Fig. 5. Process of ICE identification method.

The process of the ICE method is illustrated in Fig. 5. With the same number of generalized coordinates, the computational cost of this method may be higher than that of the ED

and EED methods because, in each load case, the FE analysis may require several iterations to achieve convergent results. In this method, all unknown stiffness coefficients are determined simultaneously instead of in small groups like the ED and EED methods. The amplitude of the applied force also influences the identified stiffness coefficients [93, 94]. Recently, higher-order polynomials, up to the eleventh order, have been considered for ICE ROMs to enhance the ability to predict the behavior of the structure when subjected to an extremely high magnitude load [94–98]. Further details of this method can be found in the Refs. [1, 87, 88].

3.3.3 Challenges

Accurately predicting the geometrically nonlinear displacements of cantilever structures poses a significant challenge for ROMs constructed using commercial FE software. This challenge arises from the unique characteristics of cantilever structure displacements. In the case of a cantilever beam subjected to a moderate-magnitude transverse load, the out-of-plane displacement of the beam exhibits near linearity, while the in-plane displacement displays a high degree of nonlinearity. Nonlinearity in the out-of-plane displacement only becomes apparent when the magnitude of the applied load is sufficiently high.

For flat cantilever structures subjected to transverse loads, Wang et al. [99] proposed a strategy to improve the accuracy of the stiffness coefficients of the ROM. First, it is necessary to separate the pure membrane displacement from the pure bending displacement. This separation is feasible for flat structures because one can easily choose the basis vectors that represent either the pure bending mode or the pure membrane mode. Then, according to Ref. [100], the stiffness coefficients represented in Eq. (33) should be eliminated, with subscripts b and m denoting the bending and membrane modes, respectively. Subsequently, the remaining stiffness coefficients can be further corrected to enhance the accuracy of the ROM [85, 99]. This strategy can also be applied to slightly curved structures, as it is also possible to identify the dominant bending modes and dominant membrane modes.

$$K^{(3)}_{bbmm} = K^{(3)}_{mmbb} = K^{(3)}_{bmbm} = K^{(3)}_{mbmb} = K^{(3)}_{bmmb} = K^{(3)}_{mbbm} = 0 . \quad (33)$$

When comparing a clamped-clamped beam and a cantilever beam of the same material and dimensions, both subjected to an identical transverse load, it becomes evident that the cantilever beam exhibits a significantly lower ratio of axial internal force to membrane displacement compared to the clamped-clamped beam. Consequently, it is reasonable to reduce the higher-order stiffness coefficients associated with membrane displacement in the case of cantilever structures. However, this strategy may prove less effective when the cantilever beam experiences simultaneous transverse and axial loads. Additionally, for structures with high curvature, this strategy may also be less effective due to the strong coupling between membrane and bending displacements present in each of the basis vectors.

4. Combining component mode synthesis and model order reduction

4.1 Overview of combination

There are three possibilities to combine the component mode synthesis with model order reduction technique as follows:

Combination 1: Component mode synthesis and explicit ROM;

Combination 2: Component mode synthesis and displacement-based identified ROM;

Combination 3: Component mode synthesis and force-based identified ROM.

Combination 1 offers the advantage of simplicity and ease of implementation. It also has the capability to enhance the accuracy of the ROM by increasing the order of the polynomial representing the internal force. However, its drawback lies in its higher computational cost compared to the other two combinations. Therefore, it is best suited for predicting the dynamic behavior of structures with complex geometries, such as curved structures, where high prediction accuracy is required.

Combination 2 offers the advantage of lower computational cost compared to combination 1. However, its limitation lies in the inability to increase the order of the polynomial representing the internal force. Therefore, it is best suited for predicting the dynamic behavior of flat or shallowly curved structures with boundary conditions that constrain membrane displacement, such as plates being clamped at all edges.

Combination 3 offers the advantage of flexibility in assuming the function representing the internal force. However, its limitation lies in considering only a limited number of eigenvectors in the reduction base. Consequently, the reduction base fails to capture the displacements of structures with complex geometries, such as curved structures. Hence, it is best suited for predicting the dynamic behavior of flat structures with boundary conditions that do not constrain membrane displacements, such as flat cantilever panels.

The subsequent Subsec. 4.2 and 4.3, present the assembly of linear and nonlinear ROMs, respectively, using the Craig-Bampton component mode synthesis technique.

4.2 Assembly of linear ROMs

The linear equation of motion for the assembled entire structure is as follows [1]:

$$\mathbf{M}_{sys}\ddot{\mathbf{q}}_{sys} + \mathbf{K}_{sys}\mathbf{q}_{sys} = \mathbf{f}_{sys} , \quad (34)$$

in which the stiffness and mass matrices of the entire structure are calculated as follows [1]:

$$\mathbf{M}_{sys}=\mathbf{L}^{T}\begin{bmatrix}\bar{\mathbf{M}}_{s,1} & \mathbf{0} & \mathbf{0} & \mathbf{0}\\ \mathbf{0} & \bar{\mathbf{M}}_{s,2} & \mathbf{0} & \mathbf{0}\\ \mathbf{0} & \mathbf{0} & \ddots & \mathbf{0}\\ \mathbf{0} & \mathbf{0} & \mathbf{0} & \bar{\mathbf{M}}_{s,n_s}\end{bmatrix}\mathbf{L}\,, \tag{35}$$

$$\mathbf{K}_{sys}=\mathbf{L}^{T}\begin{bmatrix}\bar{\mathbf{K}}_{s,1} & \mathbf{0} & \mathbf{0} & \mathbf{0}\\ \mathbf{0} & \bar{\mathbf{K}}_{s,2} & \mathbf{0} & \mathbf{0}\\ \mathbf{0} & \mathbf{0} & \ddots & \mathbf{0}\\ \mathbf{0} & \mathbf{0} & \mathbf{0} & \bar{\mathbf{K}}_{s,n_s}\end{bmatrix}\mathbf{L}\,, \tag{36}$$

where $\bar{\mathbf{M}}_{s,i}$ and $\bar{\mathbf{K}}_{s,i}$ represent the reduced-order stiffness and mass matrices of the i^{th} substructure, respectively. n_s is the number of substructures in the system. **L** is the Boolean localization matrix, which combines the connecting forces ($\mathbf{g}_s$) on both sides of each interface in such a way that they mutually cancel each other out, as follows [1]:

$$\mathbf{L}^{T}\begin{bmatrix}\begin{bmatrix}\bar{\mathbf{f}}^{B}_{s,1}+\bar{\mathbf{g}}_{s,1}\\ \bar{\mathbf{f}}^{I}_{s,1}\end{bmatrix}\\ \vdots\\ \begin{bmatrix}\bar{\mathbf{f}}^{B}_{s,n_s}+\bar{\mathbf{g}}_{s,n_s}\\ \bar{\mathbf{f}}^{I}_{s,n_s}\end{bmatrix}\end{bmatrix}=\begin{bmatrix}\bar{\mathbf{f}}^{B}_{s,1}\\ \vdots\\ \bar{\mathbf{f}}^{B}_{s,n_i}\\ \bar{\mathbf{f}}^{I}_{s,1}\\ \vdots\\ \bar{\mathbf{f}}^{I}_{s,n_s}\end{bmatrix}=\mathbf{f}_{sys}\,, \tag{37}$$

where n_i is the number of interfaces in the system. The matrix **L** also serves as the mapping of the DOFs in each substructure to the DOFs in the system, ensuring the uniqueness of each DOF, as follows [1]:

$$\begin{bmatrix}\begin{bmatrix}\mathbf{u}^{B}_{s,1}\\ \mathbf{q}^{I}_{s,1}\end{bmatrix}\\ \vdots\\ \begin{bmatrix}\mathbf{u}^{B}_{s,n_s}\\ \mathbf{q}^{I}_{s,n_s}\end{bmatrix}\end{bmatrix}=\mathbf{L}\mathbf{q}_{sys}=\mathbf{L}\begin{bmatrix}\mathbf{u}^{B}_{s,1}\\ \vdots\\ \mathbf{u}^{B}_{s,n_i}\\ \mathbf{q}^{I}_{s,1}\\ \vdots\\ \mathbf{q}^{I}_{s,n_s}\end{bmatrix}. \tag{38}$$

For example, if a structure is divided into two substructures, **L** is the mapping from the DOFs of the two substructures to the DOFs of the entire structure, as follows:

$$\begin{bmatrix}\mathbf{u}^{B}_{s}\\ \mathbf{q}^{I}_{s,1}\\ \mathbf{u}^{B}_{s}\\ \mathbf{q}^{I}_{s,2}\end{bmatrix}=\mathbf{L}\begin{bmatrix}\mathbf{u}^{B}_{s}\\ \mathbf{q}^{I}_{s,1}\\ \mathbf{q}^{I}_{s,2}\end{bmatrix}. \tag{39}$$

Therefore, L is determined as follows:

$$\mathbf{L}=\begin{bmatrix}\mathbf{I} & \mathbf{0} & \mathbf{0}\\ \mathbf{0} & \mathbf{I} & \mathbf{0}\\ \mathbf{I} & \mathbf{0} & \mathbf{0}\\ \mathbf{0} & \mathbf{0} & \mathbf{I}\end{bmatrix}. \tag{40}$$

Then, Eq. (34) can be solved using an implicit Newmark scheme for the time integration [51].

4.3 Assembly of nonlinear ROMs

The nonlinear equation of motion for the assembled entire structure is as follows [1]:

$$\mathbf{M}_{sys}\ddot{\mathbf{q}}_{sys}+\mathbf{K}_{sys}\mathbf{q}_{sys}+\mathbf{\Gamma}_{sys}\left(\mathbf{q}_{sys}\right)=\mathbf{f}_{sys}\,, \tag{41}$$

in which $\mathbf{\Gamma}$ represents the nonlinear component of internal force.

To solve Eq. (41), an implicit Newmark scheme combined with a Newton-Raphson iteration is employed [51]. The Newton-Raphson iteration is performed in each time step until convergence is achieved. At each iteration, the internal force vector and the tangent stiffness matrix require updating, as demonstrated below [1]:

$$\mathbf{f}_{\mathrm{int},red,sys}=\mathbf{L}^{T}\begin{bmatrix}\mathbf{f}_{\mathrm{int},red,1}\\ \vdots\\ \mathbf{f}_{\mathrm{int},red,n_s}\end{bmatrix}, \tag{42}$$

$$\mathbf{K}^{t}_{sys}=\mathbf{L}^{T}\begin{bmatrix}\mathbf{K}^{t}_{s,1} & \mathbf{0} & \mathbf{0} & \mathbf{0}\\ \mathbf{0} & \mathbf{K}^{t}_{s,2} & \mathbf{0} & \mathbf{0}\\ \mathbf{0} & \mathbf{0} & \ddots & \mathbf{0}\\ \mathbf{0} & \mathbf{0} & \mathbf{0} & \mathbf{K}^{t}_{s,n_s}\end{bmatrix}\mathbf{L}\,, \tag{43}$$

where the tangent stiffness matrix of the i^{th} substructure is calculated as follows:

$$\mathbf{K}^{t}_{s,i}=\mathbf{K}^{(1)}_{s,i}+2\mathbf{K}^{(2)}_{s,i}\mathbf{q}_{s,i}+\mathbf{K}^{(3)}_{s,i}\mathbf{q}_{s,i}\mathbf{q}_{s,i}+\cdots\,. \tag{44}$$

5. Conclusions

This paper has provided a comprehensive review of the combination of fixed-interface substructuring and non-intrusive model order reduction. This combination enables the creation of equivalent models for substructures, which accurately predict the mechanical behavior without requiring detailed geometric and material information. The use of equivalent models promotes safe sharing and collaboration between companies, leading to shorter design times and reduced production costs. Additionally, the reduction in computational time is a significant advantage of this approach.

However, the major challenge faced by equivalent models lies in accurately predicting the mechanical behavior of structures with high curvature and/or large rigid rotations. In such cases, a fifth-order equivalent model may yield more accurate results compared to a third-order equivalent model. Currently, the calculation of stiffness tensors for the fifth-order equivalent model involves high computational costs, as they are derived from derivatives of the stiffness matrix or internal force vector.

Therefore, it is imperative to develop methods that can efficiently identify the stiffness tensors of the fifth-order equivalent model, thereby reducing computation time.

Furthermore, improvements can be made to the reduction base and interface reduction process employed in the equivalent model. Through a comparison of reduction bases in Sec. 3.2, it is evident that creating a compact reduction base capable of handling a wide range of loads will significantly reduce the time required for building the equivalent model. Moreover, the current interface reduction process is somewhat cumbersome, and there is a need for improvements to make it more convenient and user-friendly. Finally, the accuracy of the equivalent model constructed by different combinations of component mode synthesis and nonlinear model order reduction needs to be evaluated in future studies.

Acknowledgments

The authors gratefully acknowledge the funding provided by the National Research Foundation of South Korea (NRF) [RS-2023-00246518, 25 %], the MSIT (Ministry of Science and ICT), Korea, under the Innovative Human Resource Development for Local Intellectualization program [IITP-2024-2020-0-01612, 25 %] supervised by the IITP (Institute for Information & communications Technology Planning & Evaluation), and the Korea Evaluation Institute of Industrial Technology (KEIT), and the Ministry of Trade, Industry & Energy (MOTIE, Korea) of the Republic of Korea (RS-2023-00262421, 50 %).

Nomenclature

$\boldsymbol{M}$	: Mass matrix
$\boldsymbol{K}$	: Stiffness matrix
$\boldsymbol{u}$	: Nodal displacement vector
$\boldsymbol{\ddot{u}}$	: Nodal acceleration vector
$\boldsymbol{f}$	: External force
$\boldsymbol{g}$	: Connecting force
$\boldsymbol{V}$	: Reduction basis
$\boldsymbol{q}$	: Vector consisting of generalized coordinates
$\boldsymbol{\Psi}$	: Matrix consisting of constraint modes
$\boldsymbol{\Phi}$	: Matrix consisting of vibration modes
$\boldsymbol{\Phi}^{CC}$	: Matrix consisting of characteristic constraint modes
$\boldsymbol{\Phi}^{POD}$	: Matrix consisting of proper orthogonal modes
$\boldsymbol{\Theta}$	: Matrix consisting of static modal derivatives
$\boldsymbol{f}_{int}$	: Internal force
L	: Boolean localization matrix
$\boldsymbol{I}$	: Identity matrix
n_s	: Number of substructures
n_i	: Number of interfaces

References

[1] M. S. Allen et al., *Substructuring in Engineering Dynamics*, Springer International Publishing, Cham, Switzerland (2020).

[2] D. de Klerk, D. J. Rixen and S. N. Voormeeren, General framework for dynamic substructuring: history, review and classification of techniques, *AIAA Journal*, 46 (5) (2008) 1169-1181.

[3] Z. Hao, Y. Ju and L. Chen, The use of aluminium and magnesium alloys in automotive lightweight technologies, *Journal of Mechanical Science and Technology*, 37 (9) (2023) 4615-4622.

[4] Y. Shangguan et al., Light-weight design for the aluminum alloy-carbon fiber hybrid structure of the EMU car body, *Journal of Mechanical Science and Technology*, 37 (12) (2023) 6441-6452.

[5] X. Shi et al., Stochastic dynamics analysis of the rocket shell coupling system with circular plate fasteners based on spectro-geometric method, *Compos Struct*, 329 (2024) 117727.

[6] W. C. Hurty, Dynamic analysis of structural systems using component modes, *AIAA Journal*, 3 (4) (1965) 678-685.

[7] R. R. Craig and M. C. C. Bampton, Coupling of substructures for dynamic analyses, *AIAA Journal*, 6 (7) (1968) 1313-1319.

[8] R. R. Craig and C.-J. Chang, Free-interface methods of substructure coupling for dynamic analysis, *AIAA Journal*, 14 (11) (1976) 1633-1635.

[9] Ch. U. A. Bucher, A modal synthesis method employing physical coordinates, free component modes, and residual flexibilities, *Comput Struct*, 22 (4) (1986) 559-564.

[10] R. H. MacNeal, A hybrid method of component mode synthesis, *Comput Struct*, 1 (4) (1971) 581-601.

[11] D.-M. Tran, Component mode synthesis methods using partial interface modes: Application to tuned and mistuned structures with cyclic symmetry, *Comput Struct*, 87 (17-18) (2009) 1141-1153.

[12] M. Remedia, G. S. Aglietti and G. Richardson, A stochastic methodology for predictions of the environment created by multiple microvibration sources, *J. Sound Vib*, 344 (2015) 138-157.

[13] J. H. Lim et al., A coupled dynamic loads analysis of satellites with an enhanced craig–bampton approach, *Aerosp Sci. Technol*, 69 (2017) 114-122.

[14] M. Fang, J. Wang and H. Li, An adaptive numerical scheme based on the Craig-Bampton method for the dynamic analysis of tall buildings, *The Structural Design of Tall and Special Buildings*, 27 (1) (2018) 1410.

[15] M. Junge et al., Interface-reduction for the craig-bampton and Rubin method applied to FE-BE coupling with a large fluid-structure interface, *Int. J. Numer Methods Eng.*, 77 (12) (2009) 1731-1752.

[16] P. Nachtergaele, D. J. Rixen and A. M. Steenhoek, Efficient weakly coupled projection basis for the reduction of thermo-mechanical models, *J. Comput Appl Math*, 234 (7) (2010) 2272-2278.

[17] S. Mahmoudi, F. Trivaudey and N. Bouhaddi, Benefits of metamodel-reduction for nonlinear dynamic response analysis of damaged composite structures, *Finite Elements in Analysis and Design*, 119 (2016) 1-14.

[18] J.-G. Kim and P.-S. Lee, An enhanced Craig-Bampton method, *Int. J. Numer Methods Eng.*, 103 (2) (2015) 79-93.

[19] P. V. Thomas, M. S. A. ElSayed and D. Walch, Review of model order reduction methods and their applications in aeroelasticity loads analysis for design optimization of complex airframes, *J. Aerosp Eng.*, 32 (2) (2019).

[20] I. S. Chung et al., An iterative scheme of flexibility - based component mode synthesis with higher - order residual modal compensation, *Int. J. Numer Methods Eng.*, 122 (13) (2021) 3171-3190.

[21] S. Vizzini, M. Olsson and A. Scattina, Component mode synthesis methods for a body-in-white noise and vibration analysis, *Proceedings of the Institution of Mechanical Engineers, Part D: Journal of Automobile Engineering*, 231 (2) (2017) 279-288.

[22] L. Andersson et al., Reduced order modeling of soft-body impact on glass panels, *Eng. Struct*, 256 (2022) 113988.

[23] J. B. Blaauw and J. P. Schilder, Structural analysis of a swinging fairground attraction using a novel implementation of reduced order modeling in multibody dynamics, *Eng. Struct*, 253 (2022) 113742.

[24] H. Jensen and C. Papadimitriou, *Sub-Structure Coupling for Dynamic Analysis*, Springer International Publishing, Cham, Switzerland (2019).

[25] Y. Zuo and J. Wang, A component mode synthesis method for 3-D finite element models of aero-engines, *Journal of Mechanical Science and Technology*, 29 (12) (2015) 5157-5166.

[26] S. Lee, H. Mok and C.-W. Kim, On a component mode synthesis on multi-level and its application to dynamics analysis of vehicle system supported with spring-stiffness damper system, *Journal of Mechanical Science and Technology*, 25 (12) (2011) 3115-3121.

[27] R. R. Craig, Coupling of substructures for dynamic analyses - An overview, *41st Structures, Structural Dynamics, and Materials Conference and Exhibit,* Reston, Virigina, USA (2000).

[28] Y. Sun, Y. Lu, and Z. Song, Review on the theories and applications of dynamic condensation and component mode synthesis methods in solving FEM-based structural dynamics, *Acta Mechanica Solida Sinica*, 36 (3) (2023) 361-389.

[29] R. W. Hagos and S. Chang, A review of the accuracy of primal assembly model order reduction techniques, *Multiscale Science and Engineering*, 4 (4) (2022) 179-201.

[30] R. R. J. Craig and C. J. Chang, *Substructure Coupling for Dynamic Analysis and Testing*, National Aeronautics and Space Administration, USA (1977).

[31] M. P. Castanier, Y.-C. Tan and C. Pierre, Characteristic constraint modes for component mode synthesis, *AIAA Journal*, 39 (6) (2001) 1182-1187.

[32] D. Krattiger et al., Interface reduction for Hurty/Craig-Bampton substructured models: review and improvements, *Mech. Syst. Signal Process*, 114 (2019) 579-603.

[33] P. Holzwarth and P. Eberhard, Interface reduction for CMS methods and alternative model order reduction, *IFAC-PapersOnLine*, 48 (1) (2015) 254-259.

[34] Y. Aoyama and G. Yagawa, Component mode synthesis for large-scale structural eigenanalysis, *Comput Struct*, 79 (6) (2001) 605-615.

[35] R. J. Kuether, M. S. Allen and J. J. Hollkamp, Modal substructuring of geometrically nonlinear finite element models with interface reduction, *AIAA Journal*, 55 (5) (2017) 1695-1706.

[36] S.-K. Hong, B. I. Epureanu and M. P. Castanier, Next-generation parametric reduced-order models, *Mech. Syst. Signal Process*, 37 (1-2) (2013) 403-421.

[37] E. Lindberg, N.-E. Hörlin and P. Göransson, Component mode synthesis using undeformed interface coupling modes to connect soft and stiff substructures, *Shock and Vibration*, 20 (2013) 157-170.

[38] C. Ahn et al., Refining characteristic constraint modes of component mode synthesis with residual modal flexibility, *Mech Syst Signal Process*, 178 (2022) 109265.

[39] L. Wu, P. Tiso and F. van Keulen, Interface reduction with multilevel Craig–Bampton substructuring for component mode synthesis, *AIAA Journal*, 56 (5) (2018) 2030-2044.

[40] D.-M. Tran, Component mode synthesis methods using interface modes Application to structures with cyclic symmetry, *Comput Struct*, 79 (2) (2001) 209-222.

[41] M. Karamooz Mahdiabadi et al., An augmented free-interface-based modal substructuring for nonlinear structural dynamics including interface reduction, *J. Sound Vib*, 462 (2019) 114915.

[42] E. Delhez et al., Reduced order modeling of blades with geometric nonlinearities and con-tact interactions, *J. Sound Vib*, 500 (2021) 116037.

[43] C. Touzé, A. Vizzaccaro and O. Thomas, Model order reduction methods for geometri-cally nonlinear structures: a review of nonlin-ear techniques, *Nonlinear Dyn.*, 105 (2) (2021) 1141-1190.

[44] M. P. Mignolet et al., A review of indirect/non-intrusive reduced order modeling of nonlinear geometric structures, *J. Sound Vib.*, 332 (10) (2013) 2437-2460.

[45] M. Karamooz Mahdiabadi et al., A non-intrusive model-order reduction of geometrically nonlinear structural dynamics using modal derivatives, *Mech. Syst. Signal Process*, 147 (2021) 107126.

[46] S. R. Idelsohn and A. Cardona, A reduction method for nonlinear structural dynamic analysis, *Comput Methods Appl. Mech Eng.*, 49 (3) (1985) 253-279.

[47] S. R. Idelsohn and A. Cardona, A load-dependent basis for reduced nonlinear structural dynamics, *Comput Struct*, 20 (1-3) (1985) 203-210.

[48] V. Siddhi, A generalized approach for calculation of the eigenvector sensitivity for various eigenvector normalizations, *M.S. Thesis*, University of Missouri, Missouri, USA (2005).

[49] L. Wu et al., A modal derivatives enhanced Rubin substructuring method for geometrically nonlinear multibody systems, *Multibody Syst. Dyn.*, 45 (1) (2019) 57-85.

[50] L. Wu and P. Tiso, Nonlinear model order reduction for flexible multibody dynamics: a modal derivatives approach, *Multibody Syst. Dyn.*, 36 (4) (2016) 405-425.

[51] L. Wu, Model order reduction and substructuring methods for nonlinear structural dynamics, *Ph.D. Thesis*, Delft University of Technology, Delft, Netherlands (2018).

[52] L. Wu, P. Tiso and F. van Keulen, A modal derivatives enhanced Craig-Bampton method for geometrically nonlinear

structural dynamics, *ISMA 2016 and USD 2016*, Leuven, Belgium (2016).

[53] Y.-M. Jeong and J.-S. Kim, On the stable mode selection for efficient component mode synthesis of geometrically nonlinear beams, *Journal of Mechanical Science and Technology*, 34 (7) (2020) 2961-2973.

[54] B.-S. Liao, Z. Bai and W. Gao, The important modes of subsystems: A moment-matching approach, *Int. J. Numer Methods Eng.*, 70 (13) (2007) 1581-1597.

[55] D. Givoli, P. E. Barbone and I. Patlashenko, Which are the important modes of a subsystem?, *Int. J. Numer Methods Eng.*, 59 (12) (2004) 1657-1678.

[56] P. E. Barbone, D. Givoli and I. Patlashenko, Optimal modal reduction of vibrating substructures, *Int. J. Numer Methods Eng.*, 57 (3) (2003) 341-369.

[57] H. Cho et al., Enhanced model-order reduction approach via online adaptation for parametrized nonlinear structural problems, *Comput Mech*, 65 (2) (2020) 331-353.

[58] J. Lee et al., Reduced-order modeling of nonlinear structural dynamical systems via element-wise stiffness evaluation procedure combined with hyper-reduction, *Comput Mech*, 67 (2) (2021) 523-540.

[59] K. Willcox and J. Peraire, Balanced model reduction via the proper orthogonal decomposition, *AIAA Journal*, 40 (11) (2002) 2323-2330.

[60] A. Przekop and S. A. Rizzi, Nonlinear reduced-order analysis with time-varying spatial loading distributions, *J. Aircr*, 46 (4) (2009) 1395-1402.

[61] S. A. Rizzi and A. Przekop, System identification-guided basis selection for reduced-order nonlinear response analysis, *J. Sound Vib*, 315 (3) (2008) 467-485.

[62] F. Chinesta, P. Ladeveze and E. Cueto, A short review on model order reduction based on proper generalized decomposition, *Archives of Computational Methods in Engineering*, 18 (4) (2011) 395-404.

[63] S. Im, E. Kim and M. Cho, Reduction process based on proper orthogonal decomposition for dual formulation of dynamic substructures, *Comput Mech*, 64 (5) (2019) 1237-1257.

[64] J. Cao et al., Reconstruction of full-field dynamic responses for large-scale structures using optimal sensor placement, *J. Sound Vib*, 554 (2023) 117693.

[65] T. Zhao and Y. Shen, A reduced-order peridynamic model for predicting nonlocal heat conduction in nanocomposites, *Compos Struct*, 323 (2023) 117477.

[66] E. L. Wilson, M.-W. Yuan and J. M. Dickens, Dynamic analysis by direct superposition of Ritz vectors, *Earthq Eng. Struct Dyn*, 10 (6) (1982) 813-821.

[67] L. Andersson, Reduced order modeling in structural dynamics - consideration of local nonlinearities, *Licentiate Dissertation*, Lund University, Lund, Sweden (2021).

[68] S. Voormeeren, Dynamic substructuring methodologies for integrated dynamic analysis of wind turbines, *Ph.D. Thesis*, TU Delft, Delft, Netherlands (2012).

[69] D. Rixen, High order static correction modes for component mode synthesis, *Proceedings of the Fifth World Congress on Computational Mechanics*, Vienna, Austria (2002).

[70] L. Andersson, P. Persson and K. Persson, Efficient nonlinear reduced order modeling for dynamic analysis of flat structures, *Mech. Syst. Signal Process*, 191 (2023) 110143.

[71] J. S. Han, Calculation of design sensitivity for large-size transient dynamic problems using Krylov subspace-based model order reduction, *Journal of Mechanical Science and Technology*, 27 (9) (2013) 2789-2800.

[72] J. S. Han, Efficient frequency response and its direct sensitivity analyses for large-size finite element models using Krylov subspace-based model order reduction, *Journal of Mechanical Science and Technology*, 26 (4) (2012) 1115-1126.

[73] T. A. Bui, J.-S. Kim and J. Park, Efficient method for derivatives of nonlinear stiffness matrix, *Mathematics*, 11 (7) (2023) 1572.

[74] J. Rutzmoser, Model order reduction for nonlinear structural dynamics, *Dissertation*, Technische Universität München, Munich, Germany (2018).

[75] T. A. Bui, J.-S. Kim and J. Park, Geometrically nonlinear static deflection of stiffened composite plates: a fifth-order equivalent model, *Compos Struct*, 323 (2023) 117508.

[76] A. Givois et al., On the frequency response computation of geometrically nonlinear flat structures using reduced-order finite element models, *Nonlinear Dyn*, 97 (2) (2019) 1747-1781.

[77] S. Jain, P. Tiso and G. Haller, Exact nonlinear model reduction for a von Kármán beam: Slow-fast decomposition and spectral submanifolds, *J. Sound Vib*, 423 (2018) 195-211.

[78] M. P. Mignolet and C. Soize, Stochastic reduced order models for uncertain geometrically nonlinear dynamical systems, *Comput Methods Appl. Mech Eng.*, 197 (45-48) (2008) 3951-3963.

[79] J. M. Seawright, R. Wiebe and R. A. Perez, Guided identification of nonlinear reduced-order models via the incorporation of von Kármán beam theory, *Int. J. Non Linear Mech*, 150 (2023) 104348.

[80] T. A. Bui, J. Park and J.-S. Kim, A reduced-order model for geometrically nonlinear curved beam structures with substructuring techniques, *Int. J. Non Linear Mech*, 162 (2024) 104724.

[81] K. Kim et al., Nonlinear reduced order modeling of isotropic and functionally graded plates, *Int. J. Non-Linear Mech*, 49 (2013) 100-110.

[82] A. A. Muravyov and S. A. Rizzi, Determination of nonlinear stiffness with application to random vibration of geometrically nonlinear structures, *Comput Struct*, 81 (15) (2003) 1513-1523.

[83] A. Matney et al., Nonlinear structural reduced order modeling methods for hypersonic structures, *53rd AIAA/ASME/ASCE/AHS/ASC Structures, Structural Dynamics and Materials Conference & 20th AIAA/ASME/AHS Adaptive Structures Conference & 14th AIAA, American Institute of Aeronautics and Astronautics*, Reston, Virigina, USA (2012).

[84] R. Perez, X. Q. Wang and M. P. Mignolet, Nonintrusive structural dynamic reduced order modeling for large deformations: enhancements for complex structures, *J. Comput Nonlinear Dyn*, 9 (3) (2014) 031008.

[85] J. Lin et al., Improved identification of stiffness coefficients of non intrusive nonlinear geometric reduced order models of structures, *Int. J. Non-Linear Mech*, 152 (2023) 104380.
[86] M. P. Mignolet and A. G. Radu, Validation of reduced order modeling for the prediction of the response and fatigue life of panels subjected to thermo-acoustic effects, *Eighth International Conference on Recent Advances in Structural Dynamics*, Southampton, UK (2003).
[87] M. I. McEwan, A combined modal/finite element technique for the non-linear dynamic simulation of aerospace structures, *Ph.D. Thesis*, University of Manchester, Manchester, UK (2001).
[88] R. W. Gordon and J. J. Hollkamp, *Reduced-Order Models for Acoustic Response Prediction*, Air Force Research Laboratory, USA (2011).
[89] J. Hollkamp and R. Gordon, Modeling membrane displacements in the sonic fatigue response prediction problem, *46th AIAA/ASME/ASCE/AHS/ASC Structures, Structural Dynamics and Materials Conference,* Reston, Virigina, USA (2005).
[90] J. J. Hollkamp, R. W. Gordon and S. M. Spottswood, Nonlinear modal models for sonic fatigue response prediction: a comparison of methods, *J. Sound Vib.*, 284 (3-5) (2005) 1145-1163.
[91] J. J. Hollkamp and R. W. Gordon, Reduced-order models for nonlinear response prediction: Implicit condensation and expansion, *J. Sound Vib.*, 318 (4-5) (2008) 1139-1153.
[92] M. McEwan et al., A finite element/modal technique for nonlinear plate and stiffened panel response prediction, *19th AIAA Applied Aerodynamics Conference*, Reston, Virigina, USA (2001).
[93] Y. Shen et al., Reduced order models for geometrically nonlinear structures: assessment of implicit condensation in comparison with invariant manifold approach, *European Journal of Mechanics - A/Solids*, 86 (2021) 104165.
[94] E. Nicolaidou et al., Accounting for quasi-static coupling in nonlinear dynamic reduced-order models, *J. Comput Nonlinear Dyn*, 15 (7) (2020) 071002.
[95] X. Xiao, T. L. Hill and S. A. Neild, Ensuring the accuracy of indirect nonlinear dynamic reduced-order models, *Nonlinear Dyn*, 112 (3) (2024) 1997-2019.
[96] E. Nicolaidou, T. L. Hill and S. A. Neild, Indirect reduced-order modelling: using nonlinear manifolds to conserve kinetic energy, *Proceedings of the Royal Society A: Mathematical, Physical and Engineering Sciences*, 476 (2243) (2020) 20200589.
[97] K. Park and M. S. Allen, Quasi-static modal analysis for reduced order modeling of geometrically nonlinear structures, *J. Sound Vib.*, 502 (2021) 116076.
[98] A. Frangi and G. Gobat, Reduced order modelling of the nonlinear stiffness in MEMS resonators, *Int. J. Non Linear Mech*, 116 (2019) 211-218.
[99] X. Q. Wang et al., Nonlinear reduced-order modeling of flat cantilevered structures: Identification challenges and remedies, *J. Aerosp Eng.*, 34 (6) (2021) 04021085.
[100] X. Q. Wang, M. P. Mignolet and C. Soize, Structural uncertainty modeling for nonlinear geometric response using nonintrusive reduced order models, *Probabilistic Engineering Mechanics*, 60 (2020) 103033.

Tuan Anh Bui is a post doctor of the Department of Aeronautic, Mechanical and Electrical Convergence Engineering, Kumoh National Institute of Technology, Gumi, Korea. He received his Ph.D. in Energy and Mechanics from the University of Lorraine, France. His research interests include vibration, geometric nonlinearity and model order reduction.

Junyoung Park is a Professor of the Department of Aeronautic, Mechanical and Electrical Convergence Engineering, and the School of Mechanical System Engineering, Kumoh National Institute of Technology, Gumi, Korea. He received his Ph.D. in Mechanical Engineering from the Purdue University, USA. His research interests include discrete element method, evacuation modeling, molecular dynamics, wind power and power systems, and powder technology.

Jun-Sik Kim is a Professor of the Department of Aeronautic, Mechanical and Electrical Convergence Engineering, and the School of Mechanical System Engineering, Kumoh National Institute of Technology, Gumi, Korea. He received his Ph.D. in Aerospace Engineering from the Pennsylvania State University, USA. His research interests include solid mechanics, computational mechanics, smart structures, and helicopter dynamics.